

# Strain engineering magnetic frustration in perovskite oxide thin films

Carlos Escorihuela-Sayalero, Oswaldo Diéguez, and Jorge Íñiguez

*Institut de Ciència de Materials de Barcelona (ICMAB-CSIC), Campus UAB, 08193 Bellaterra, Spain*

Our first-principles results show that geometric frustration can be induced in thin films of multi-ferroic BiFeO<sub>3</sub>. We find that competing magnetic interactions occur in the so-called *super-tetragonal* phase of this material, which can be grown on strongly-compressive substrates. We show that the frustration level can be *tuned* by appropriately choosing the substrate; in fact, the three-dimensional spin order gets totally annihilated in a narrow range of epitaxial strains. We argue that the effects revealed here are not exclusive to BiFeO<sub>3</sub>, and predict that they also occur in multiferroic BiCoO<sub>3</sub>.

PACS numbers: 75.85.+t, 71.15.Mb, 77.80.Bn, 71.15.Mb

The competition between different interactions underlies some of the most fascinating phenomena in condensed-matter physics. When the competing orders are of similar strength, rich phase diagrams are likely to emerge, and the materials tend to be strongly responsive to external perturbations. Examples abound in the family of perovskite oxides, ranging from magnetoresistive manganites [1] to ferroelectric relaxors [2, 3]. In addition to the fascinating science they involve, competing interactions often lead to important functionalities.

Of special interest are the cases in which the competition relies on the topology of the crystal lattice, as in a triangular network of anti-ferromagnetically coupled spins, which is the classic example of *geometric frustration*. Here we present first-principles results showing that *strain engineering* (i.e., taking advantage of the mismatch stress exerted by a substrate on a thin film) can be used to induce a novel kind of *tunable* geometric frustration in a spin system. Our work focuses on room-temperature multiferroic BiFeO<sub>3</sub>, and we show that the same effects also occur in other compounds like BiCoO<sub>3</sub>.

*Tunable frustration in BiFeO<sub>3</sub>.*— Multiferroic BiFeO<sub>3</sub> (BFO) is a perovskite oxide that presents ferroelectric ( $T_C \approx 1100$  K) and magnetic ( $T_N \approx 760$  K) orders at ambient conditions [4]. While the usual BFO phase is rhombohedral ( $R3c$  space group), it was recently discovered that BFO's atomic structure can be drastically modified by growing thin films on strongly compressive (001)-oriented substrates [5]. The phases thus obtained are called *super-tetragonal* (*ST*), as their (pseudo-cubic) unit cell presents a very large aspect ratio  $c/a \approx 1.25$  (see Fig. 1). Such *ST*-BFO phases display a number of appealing features and are currently receiving a lot of attention; in particular, they undergo both structural and magnetic-ordering transitions slightly above room temperature ( $T_r$ ) [6, 7], which might lead to improved functional properties.

The magnetic order of *ST*-BFO remains an open problem. Several first-principles works [8, 9] predict the so-called C-type anti-ferromagnetic (C-AFM) spin arrangement, while most experimental studies suggest that the so-called G-AFM order dominates [5, 10]. As shown in Fig. 1, the C-AFM and G-AFM orders are identi-

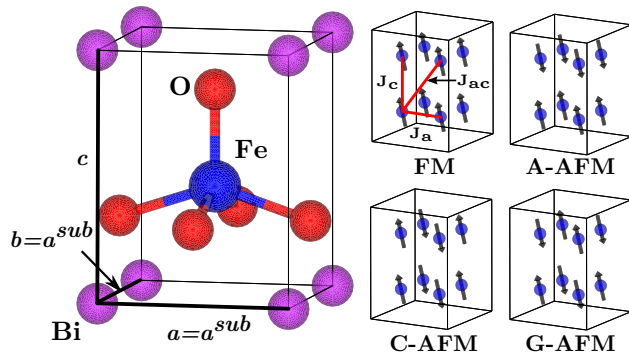


FIG. 1. (Color online.) Left: Elemental 5-atom cell of *ST*-BFO, indicating the in-plane epitaxial constraint  $a = b = a^{\text{sub}}$ . Right: Spin arrangements considered in this work. We sketch the  $2 \times 2 \times 2$  repetition of the elemental cell that we simulated, showing only the Fe atoms. In the FM case we indicate the exchange interactions  $J$  discussed in the text.

cal within the  $ab$  plane (first-neighboring spins are anti-parallel), but differ along the out-of-plane  $z$  direction (first-neighboring spins are parallel in C-AFM and anti-parallel in G-AFM). It is generally accepted [6, 8–11] that the in-plane exchange interaction between neighboring Fe atoms ( $J_a$  in Fig. 1) is anti-ferromagnetic and relatively strong; in contrast, the out-of-plane couplings ( $J_c$  and  $J_{ac}$  in Fig. 1) are believed to be small because of the very large separation between irons along the  $z$  direction. In fact, MacDougall *et al.* [10] have argued that the occurrence of C-AFM or G-AFM orders in specific films may be decided by factors that would be *extrinsic* to a perfect *ST*-BFO lattice, as the *intrinsic* out-of-plane couplings can be expected to be negligible.

Wanting to shed light on these issues, we used first-principles methods [12, 13] to investigate the magnetic order in *ST*-BFO as a function of the epitaxial strain exerted by a (001)-oriented square substrate. For this purpose, we considered a perfectly tetragonal atomic structure ( $P4mm$  space group); we checked that, as regards the spin couplings, this structure is representative of the variety of lower-symmetry (monoclinic) phases [9, 14] that occur in the actual films. For each considered value of the substrate lattice parameter  $a^{\text{sub}}$  [15], we stud-

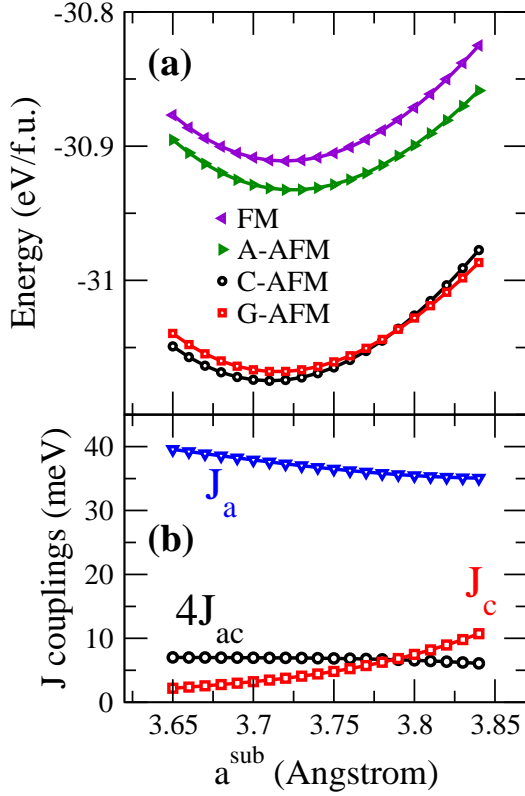


FIG. 2. (Color online.) Panel (a): Energies of the different spin arrangements as a function of  $a^{\text{sub}}$ . Panel (b): Exchange constants defined in Fig. 1 as a function of  $a^{\text{sub}}$ .  $J_{ac}$  is multiplied by 4, to better visualize the point at which  $E_G = E_C$ .

ied several spin arrangements (FM, A-AFM, C-AFM, and G-AFM, sketched in Fig. 1); for each arrangement, we relaxed the atomic structure subject to the epitaxial constraint. As shown in Fig. 2(a), we find that the C-AFM arrangement is the lowest-energy solution for the most stable films, which correspond to  $a^{\text{sub}} \approx 3.71$  Å. The G-AFM order gets stabilized as  $a^{\text{sub}}$  increases, the transition between C-AFM and G-AFM occurring at  $a^{\text{sub}} \approx 3.79$  Å.

To gain more insight, let us consider the Heisenberg spin Hamiltonian  $E - E_0 = 1/2N \sum_{i \neq j} J_{ij} \mathbf{S}_i \cdot \mathbf{S}_j$ , where  $N$  is the total number of Fe atoms, needed to capture such a crossover. Let us assume classical spins and take  $|\mathbf{S}_i| = 1$  for simplicity. Then, if we restrict ourselves to couplings between first-nearest neighbors (i.e., to  $J_a$  and  $J_c$  in Fig. 1, as discussed by other authors [8, 10]), the energies per Fe atom of the C-AFM and G-AFM orders are  $E_C = E_0 - 2J_a - J_c$  and  $E_G = E_0 - 2J_a + J_c$ , respectively. The crossover point ( $E_G = E_C$ ) would thus correspond to  $J_c = 0$ , i.e., to the value of  $a^{\text{sub}}$  at which  $J_c$  changes sign. However, this simple model is not satisfactory, for two main reasons: (1) It is difficult to imagine an exchange mechanism that may render a ferromagnetic (FM) coupling  $J_c < 0$ . Indeed, the  $J_c$  coupling is associ-

ated to a  $\text{Fe}^{3+}-\text{O}^{2-}-\text{Fe}^{3+}$  chain forming a  $180^\circ$  angle, for which the well-known Goodenough-Kanamori rules [16] predict an AFM super-exchange interaction; such an expectation should hold even in a case like this one, where the two Fe-O bonds in the super-exchange path have different lengths. (2) For  $J_c < 0$ , such a simple model predicts  $E_C < E_G < E_F < E_A$ . However, our results show that the FM order is the least favorable one throughout the considered  $a^{\text{sub}}$  range. Indeed, our calculations predict that, even though there is a crossover between the C-AFM and G-AFM orders, where the magnetic interaction between  $ab$  layers changes sign, the analogous crossover between FM and A-AFM does not take place!

These difficulties are resolved by extending the model in the simplest possible way, i.e., by including the  $J_{ac}$  interaction defined in Fig. 1. The energies per Fe atom of our four magnetic orders are then given by:

$$E_F = E_0 + 2J_a + J_c + 4J_{ac}, \quad (1)$$

$$E_A = E_0 + 2J_a - J_c - 4J_{ac}, \quad (2)$$

$$E_C = E_0 - 2J_a + J_c - 4J_{ac}, \quad (3)$$

$$E_G = E_0 - 2J_a - J_c + 4J_{ac}. \quad (4)$$

We can thus compute the  $J$ 's from the data in Fig. 2(a); the results are shown in Fig. 2(b). This extended model is able to reproduce exactly the first-principles energies of our four magnetic structures in the whole  $a^{\text{sub}}$  range. In addition, the obtained values of  $J_c$  and  $J_{ac}$  are always positive, which corresponds to AFM interactions; as regards  $J_c$ , this is compatible with the expectations from the Goodenough-Kanamori analysis.

It may seem surprising that this model can capture the C-AFM ground state, given that the computed out-of-plane interactions,  $J_c$  and  $J_{ac}$ , are both AFM in nature. To understand this, let us consider first what determines the relative stability of the FM and A-AFM orders, for which we have  $E_F - E_A = 2J_c + 8J_{ac}$ . Here, in both cases the  $ab$  planes are ferromagnetically ordered, and both  $J_c$  and  $J_{ac}$  favor the A-AFM solution over the FM one. On the other hand, the energy gap between C-AFM and G-AFM is  $E_C - E_G = 2J_c - 8J_{ac}$ . In this case, the  $ab$  planes are anti-ferromagnetically ordered, and the out-of-plane interactions compete: A positive  $J_c$  favors the G-AFM order via the AFM coupling between Fe ions that are first neighbors out-of-plane. In contrast, a positive  $J_{ac}$  favors the C-AFM order via the AFM coupling between Fe ions that are second neighbors out-of-plane. When  $J_{ac}$  is large enough – i.e., when  $4J_{ac} > J_c$ , where the factor of 4 comes from the ratio between first- and second-nearest neighbors out-of-plane –, the C-AFM order prevails. Hence, according to this model, the predicted stabilization of the C-AFM phase relies on both the AFM interaction  $J_{ac}$  and the presence of a robust AFM order within the  $ab$  planes.

The obtained  $a^{\text{sub}}$ -dependence of the exchange constants  $J_a$  and  $J_c$  seems rather natural. As we compress

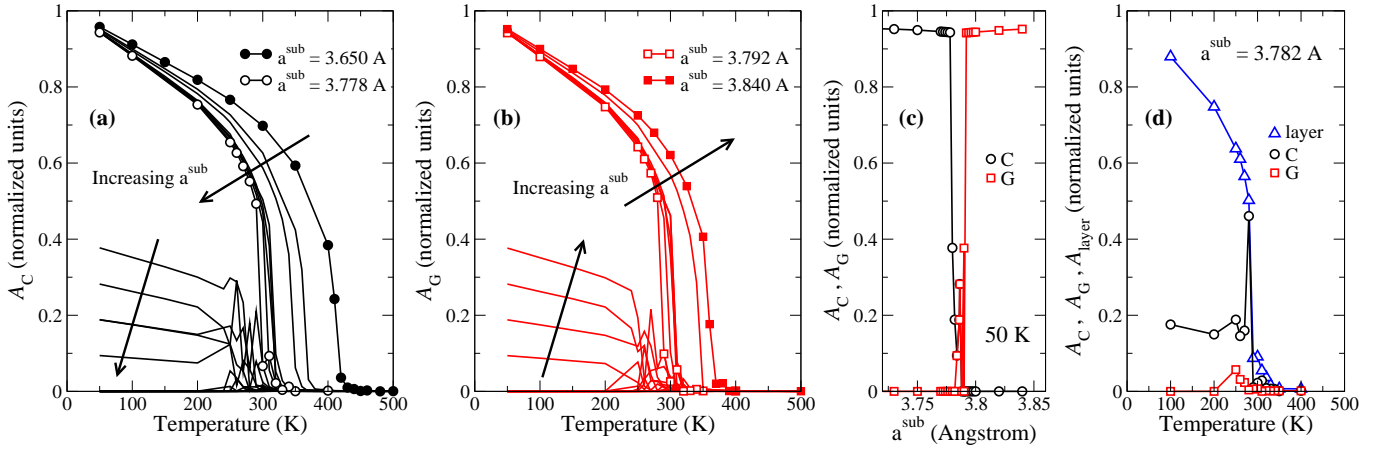


FIG. 3. (Color online.) Results from Monte Carlo simulations. Panels (a) and (b):  $T$ -dependence of the order parameters quantifying the degree of C-AFM ( $A_C$ ) and G-AFM ( $A_G$ ) order, respectively. We show the results for all the substrates investigated, with  $a^{\text{sub}}$  ranging from 3.65 Å to 3.84 Å.  $A_s = N^{-1} \sum_j S_{jz} \exp(i\mathbf{q}_s \mathbf{R}_j)$ , where  $N$  is the number of cells in the simulation box and  $\mathbf{R}_j$  is the lattice vector corresponding to spin  $\mathbf{S}_j$ ;  $\mathbf{q}_s$  defines the  $s$ -like spin arrangement, with  $\mathbf{q}_C = 2\pi/a^{\text{sub}}(1/2, 1/2, 0)$  and  $\mathbf{q}_G = 2\pi(1/2a^{\text{sub}}, 1/2a^{\text{sub}}, 1/2c)$ . We only need to consider the  $z$  component of the spins ( $S_{jz}$ ) because of the small symmetry-breaking included in our Hamiltonians [17]. A perfect  $s$ -like order corresponds to having  $A_s = 1$ . Panel (c):  $A_C$  and  $A_G$  obtained at 50 K and as a function of  $a^{\text{sub}}$ . Panel (d): results for  $a^{\text{sub}} = 3.782$  Å.  $A_{\text{layer}}$  quantifies the AFM order within the  $ab$  layers.  $A_{\text{layer}} = N_{\text{layer}}^{-1} \sum_j S_{jz} \exp(i\mathbf{q}_{2D} \mathbf{R}_j)$ , where the primed sum runs over the spins in the first  $ab$  layer, which is representative of the rest;  $N_{\text{layer}}$  is the number of cells in a layer and  $\mathbf{q}_{2D} = 2\pi/a^{\text{sub}}(1/2, 1/2, 0)$ .

in-plane, the Fe spins coupled by  $J_a$  get closer and their interaction becomes stronger; in contrast, the distance between irons coupled by  $J_c$  grows (results in [13]) and the interaction weakens [18]. However, it is not clear what to expect for  $J_{ac}$ . In this case, any coupling mechanism that one can imagine will have both in-plane and out-of-plane *components*; hence, it is probably not surprising to find that  $J_{ac}$  varies weakly with  $a^{\text{sub}}$ .

Hence, our calculations and model analysis reveal a robust mechanism leading to a crossover between G-AFM and C-AFM orders as  $a^{\text{sub}}$  varies. Such a transition is the result of the competition between two magnetic interactions that become comparable in a certain range of epitaxial strains. In fact, our *ST*-BFO films can be considered a case of *frustrated spin system*, where the magnitude of the frustration can be *tuned* by appropriately choosing the substrates on which the films are grown.

*Phase diagram.*— We solved our Hamiltonians by performing Monte Carlo simulations in a periodically-repeated box of  $20 \times 20 \times 20$  spins [19, 20]. Figures 3(a) and 3(b) show, respectively, our results for the  $T$ -dependence of the parameters monitoring the C-AFM ( $A_C$ ) and G-AFM ( $A_G$ ) orders; Fig. 3(c) shows the results for  $T = 50$  K, where the evolution of the ground state with  $a^{\text{sub}}$  is easily appreciated [17].

Our simulations render a paramagnetic (PM) phase at high temperatures. Then, for  $a^{\text{sub}} \leq 3.778$  Å we observe a transition to a C-AFM phase as  $T$  decreases; in contrast, for  $a^{\text{sub}} \geq 3.792$  Å the low- $T$  phase presents the G-AFM spin order. In the narrow intermediate region  $3.778 \text{ Å} < a^{\text{sub}} < 3.792 \text{ Å}$ , some sort of  $T$ -driven tran-

sition occurs as evidenced by the non-zero values of  $A_G$  and  $A_C$ ; however, no clear-cut three-dimensional order emerges.

Figure 3(d) shows results for  $a^{\text{sub}} = 3.782$  Å, which is representative of the intermediate region. In this case,  $A_G$  and  $A_C$  take values that look rather arbitrary. Nevertheless, if we consider the AFM order within the  $ab$  planes, as quantified by  $A_{\text{layer}}$  defined in the figure caption, we recover a well-behaved transition. The picture that emerges is thus clear: For intermediate values of  $a^{\text{sub}}$  the system becomes *two-dimensional* (2D). The out-of-plane correlations are very weak, and long-range order along  $z$  essentially disappears.

Figure 4 shows the phase diagram that emerges from our results. Note that the width of the 2D region depends on the specific box size and sampling method used in our simulations. Indeed, for small but non-zero values of  $|J_c - 4J_{ac}|$ , the ground state of the system is well defined in the thermodynamic limit. However, the specifics of our simulations will determine whether the AFM planes can order *correctly* along the  $z$  direction or, instead, get stuck in a meta-stable configuration displaying disorder and/or phase co-existence. [As appreciated in Fig. 3(c), we tend to find incomplete G-like (resp. C-like) order on the right (left) side of the intermediate region, which is a result of having  $J_c - 4J_{ac} \gtrsim 0$  (resp.  $J_c - 4J_{ac} \lesssim 0$ ).] Hence, the 2D region in Fig. 4 has to be taken as evidence for what probably is a *line* separating the C-AFM and G-AFM phases in the ideal case.

In order to understand the evolution of  $T_N$  with  $a^{\text{sub}}$ , it is useful to resort to a mean-field (MF) analysis of our

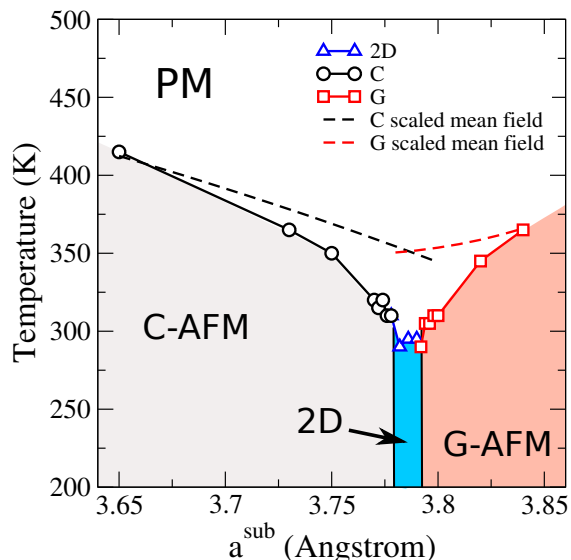


FIG. 4. (Color online.) Phase diagram deduced from our Monte Carlo simulation. The dashed lines show the transition lines obtained at the mean-field level, which are rescaled to fit with the Monte Carlo results (see text).

Hamiltonians. Within this approximation, the transition temperature is proportional to the *mean field* experienced by the spins in the lattice; such a field is essentially given by  $4J_a - 2J_c + 8J_{ac}$  in the C-AFM case, and by  $4J_a + 2J_c - 8J_{ac}$  for the G-AFM solution. In Fig. 4 we plot the  $a^{\text{sub}}$ -dependence of these MFs; note that we multiply the results by a factor that is constant through the whole  $a^{\text{sub}}$  range and common to both spin arrangements, so that the MF lines fit in the scale of the Monte Carlos results. As we can see, the general dependence of  $T_N$  with  $a^{\text{sub}}$  is captured at the MF level. In particular, for decreasing  $a^{\text{sub}}$  values,  $T_N$  of the PM→C-AFM transition grows as a consequence of the increasing in-plane coupling  $J_a$ . On the other hand, if  $a^{\text{sub}}$  becomes larger,  $T_N$  of the PM→G-AFM transition grows driven by the rapidly increasing  $J_c$  interaction. Finally, as we approach the 2D region, the  $T_N$  values obtained from Monte Carlo decrease more strongly than we would predict at the MF level. This is most likely a consequence of the competition at play in the Monte Carlo simulations, as such an effect is not captured by our simple MF analysis.

*Further discussion.*— Previous works have shown that the approach adopted here renders reliable Néel temperatures for *ST*-BFO [6, 11]. Indeed, for BFO films grown on  $\text{LaAlO}_3$  ( $a^{\text{sub}} = 3.79$  Å), measured  $T_N$  values range from 324 K [10] to 360 K [6], which is in reasonable agreement with our results [21, 22].

Regarding the specific magnetic order, as far as we know only films grown on  $\text{LaAlO}_3$  have been characterized experimentally. There seems to be consensus about the fact that the films adopt a G-AFM order at  $T_r$  [5, 6, 10]. Additionally, MacDougall *et al.* [10] have

reported a coexistence of G-AFM and C-AFM orders at temperatures below 260 K. Such a situation seems compatible with the 2D region that we find precisely for  $a^{\text{sub}} \approx 3.79$  Å. Indeed, for  $J_c - 4J_{ac} \gtrsim 0$  we obtained a dominant, but not complete, G-AFM order [see Fig. 3(c)], which clearly resembles the experimental findings of Ref. 10.

At and around the 2D region we have  $J_c - 4J_{ac} \approx 0$ , which results in an effective magnetic *decoupling* of the *ab* planes. In such cases, it is conceivable that impurities, defects, and other extrinsic factors may influence the nature of the magnetic ground state or the relative populations of co-existing phases. However, for smaller  $a^{\text{sub}}$  values we obtain a sizable  $J_c - 4J_{ac} < 0$ . Hence, we predict that C-AFM order will occur in *SF*-BFO grown on substrates more compressive than  $\text{LaAlO}_3$ .

Note that this picture differs significantly from that of MacDougall *et al.* [10], who argued that all the out-of-plane couplings are essentially negligible (i.e.,  $J_c \approx 0$  and  $J_{ac} \approx 0$ ) in *ST*-BFO grown on  $\text{LaAlO}_3$ . Their interpretation implies that the magnetic order in *ST*-BFO should be 2D-like for any substrate more compressive than  $\text{LaAlO}_3$ , and one would not expect to observe any robust C-AFM phase. This is clearly at variance with our results.

How general is the tunable geometric frustration predicted in this work? Let us emphasize that the requirements to observe these effects do not seem exotic at all: In essence, we need to (1) have AFM interactions between neighboring magnetic cations, and (2) obtain an expansion of the out-of-plane lattice parameter as we compress in-plane. Condition (1) is satisfied by many perovskite oxides that are AFM insulators. Condition (2) is the expected behavior for all perovskites; further, there is a growing number of compounds that are known to display large  $c/a$  ratios when grown under appropriate conditions.

To test this presumed generality, we investigated  $\text{BiCoO}_3$  (BCO) under epitaxial strain. BCO is an insulating perovskite whose ground state has the ideal *ST* structure ( $P4mm$  space group, with  $c/a = 1.27$  and  $a = 3.73$  Å) and a C-AFM spin order [23]. As we imposed a tensile epitaxial strain, we observed a transition from C-AFM to G-AFM at  $a^{\text{sub}} \approx 3.84$  Å. As in the case of *SF*-BFO, the analogous crossover between the FM and A-AFM orders is absent, and the transition point is defined by the condition  $J_c = 4J_{ac}$ , with all the computed exchange couplings being AFM in nature. Hence, BCO presents exactly the same magnetic frustration effects that we have discussed for *ST*-BFO. Our BCO results are summarized in [13], including the prediction that G-AFM order can be obtained in BCO films at  $T_r$ . Hence, BCO, as well as the BFO-BCO solid solutions studied in Ref. 11, may offer interesting alternatives for the experimental investigation of these effects.

Work supported by MINECO-Spain through Grants

No. MAT2010-18113, No. MAT2010-10093-E, and No. CSD2007-00041, and the “Ramón y Cajal” program (OD). We made use of the computing facilities provided by CESGA and RES. M. Bibes’ comments are gratefully acknowledged.

- 
- [1] Y. Tokura and Y. Tomioka, *Journal of Magnetism and Magnetic Materials* **200**, 1 (1999).
- [2] R. Pirc and R. Blinc, *Physical Review B* **60**, 13470 (1999).
- [3] G. A. Samara, *Journal of Physics: Condensed Matter* **15**, R367 (2003).
- [4] G. Catalan and J. F. Scott, *Advanced Materials* **21**, 2463 (2009).
- [5] H. Béa, B. Dupe, S. Fusil, R. Mattana, E. Jacquet, B. Warot-Fonrose, F. Wilhelm, A. Rogalev, S. Petit, V. Cros, A. Anane, F. Petroff, K. Bouzehouane, G. Geneste, B. Dkhil, S. Lisenkov, I. Ponomareva, L. Bellaiche, M. Bibes, and A. Barthélémy, *Physical Review Letters* **102**, 217603 (2009).
- [6] I. C. Infante, J. Juraszek, S. Fusil, B. Dupé, P. Gemeiner, O. Diéguez, F. Pailloux, S. Jouen, E. Jacquet, G. Geneste, J. Pacaud, J. Íñiguez, L. Bellaiche, A. Barthélémy, B. Dkhil, and M. Bibes, *Physical Review Letters* **107**, 237601 (2011).
- [7] K. Ko, M. H. Jung, Q. He, J. H. Lee, C. S. Woo, K. Chu, J. Seidel, B. Jeon, Y. S. Oh, K. H. Kim, W. Liang, H. Chen, Y. Chu, Y. H. Jeong, R. Ramesh, J. Park, and C. Yang, *Nature Communications* **2**, 567 (2011).
- [8] A. J. Hatt, N. A. Spaldin, and C. Ederer, *Physical Review B* **81**, 054109 (2010).
- [9] O. Diéguez, O. E. González-Vázquez, J. C. Wojdel, and J. Íñiguez, *Physical Review B* **83**, 094105 (2011).
- [10] G. J. MacDougall, H. M. Christen, W. Siemons, M. D. Biegalski, J. L. Zarestky, S. Liang, E. Dagotto, and S. E. Nagler, *Physical Review B* **85**, 100406 (2012).
- [11] O. Diéguez and J. Íñiguez, *Physical Review Letters* **107**, 057601 (2011).
- [12] The first-principles methods employed are described in the online Supplementary Materials [13], and are exactly the ones used in Ref. 11.
- [13] See online Supplementary Materials accompanying this article.
- [14] H. M. Christen, J. H. Nam, H. S. Kim, A. J. Hatt, and N. A. Spaldin, *Physical Review B* **83**, 144107 (2011).
- [15] We ran first-principles calculations for  $a^{\text{sub}}$  values in a grid with  $\Delta a^{\text{sub}} = 0.01 \text{ \AA}$ . To determine the boundaries of the 2D region of Fig. 4, we ran Monte Carlo simulations for an even finer grid with  $\Delta a^{\text{sub}} = 0.002 \text{ \AA}$ ; the employed spin Hamiltonians were obtained by interpolating the results in Fig. 2(b).
- [16] D. Khomskii, in *Spin Electronics*, Lecture Notes in Physics, Vol. 569, edited by M. Ziese and M. Thornton (Springer Berlin / Heidelberg, 2001) pp. 89–116.
- [17] For the sake of convenience, we introduced a small magnetic anisotropy in the spin Hamiltonians, so that the easy axis is fixed to lie along  $z$ . Thus, in Fig. 3 we only show the  $z$  component of the three-dimensional order parameters.
- [18] The qualitative  $a^{\text{sub}}$ -dependence of  $J_a$  and  $J_c$  clearly correlates with the variation of the corresponding the Fe–Fe distances. This trivial dependence was also pointed out by MacDougall *et al.* [10] when discussing the differences in the magnetic couplings between BFO’s rhombohedral and *ST* phases. Of course, a more quantitative argument should take into account the detailed evolution of the interaction paths (e.g., the  $a^{\text{sub}}$ -dependence of the Fe–O–Fe angle in the case of  $J_a$ , and of the two different Fe–O distances in the case of  $J_c$ ).
- [19] We ran regular Metropolis Monte Carlo, performing 10000 sweeps of the full simulation box for thermalization and 50000 additional sweeps for computing averages. The algorithm to generate new spin configurations was a combination of regular sampling (typically aiming at an acceptance ratio of 40 %) and the *magic steps* described in Ref. 20. The calculation conditions were checked to render sufficiently converged results.
- [20] A. N. Rubtsov, J. Hlinka, and T. Janssen, *Physical Review E* **61**, 126 (2000).
- [21] This level of agreement probably exceeds what one may expect from magnetic interactions computed using density functional theory (DFT) methods. Yet, note that our DFT scheme, which employs a “Hubbard  $U$ ” correction with  $U = 4 \text{ eV}$  for Fe and  $U = 6 \text{ eV}$  for Co, was checked to produce magnetic couplings in good agreement with results obtained using hybrid functionals, which are known to be accurate for the calculation of such interactions in magnetic insulators. The reliability of such an  $U$ -fitting procedure has been recently shown [22].
- [22] J. Hong, A. Stroppa, J. Íñiguez, S. Picozzi, and D. Vanderbilt, *Physical Review B* **85**, 054417 (2012).
- [23] A. A. Belik, S. Iikubo, K. Kodama, N. Igawa, S. Shamoto, S. Niitaka, M. Azuma, Y. Shimakawa, M. Takano, F. Izumi, and E. Takayama-Muromachi, *Chemistry of Materials* **18**, 798 (2006).